https://doi.org/10.5194/gchron-2020-1
Preprint. Discussion started: 7 February 2020

GEOCHRONOLOGY Discussions Open Access EGU

The Isotopx NGX and the ATONA Faraday Amplifiers

Stephen E Cox[1], Sidney R Hemming[1, 2], and Damian Tootell[3]

[1]Lamont-Doherty Earth Observatory, the Earth Institute at Columbia University, 61 Route 9W, Palisades, NY 10964, USA
[2]Department of Earth and Environmental Sciences, Columbia University, New York, NY 10027, USA
[3]Isotopx, Ltd., Dalton House, Dalton Way, Middlewich CW10 0HU, UK

Correspondence: Stephen E Cox (stephen@stephencoxgeology.com))

Abstract. We installed the new Isotopx ATONA Faraday cup detector amplifiers on an Isotopx NGX mass spectrometer at Lamont-Doherty Earth Observatory in early 2018. The ATONA is a capacitive transimpedance amplifier, which differs from the traditional resistive transimpedance amplifier used on most Faraday detectors for mass spectrometry. Instead of a high gain resistor, a capacitor is used to accumulate and measure charge. The advantages of this architecture are a very low noise floor, rapid response time, stable baselines, and very high dynamic range. We show baseline noise measurements and measurements of argon from air and cocktail gas standards to demonstrate the capabilities of these amplifiers. The ATONA exhibits a noise floor better than a traditional 10^{13} Ω amplifier in normal noble gas mass spectrometer usage, superior gain and baseline stability, and an unrivaled dynamic range that makes it practical to measure beams ranging in size from below 10^{-16} A to above 10^{-9} A using a single amplifier.

1 Introduction

The design of analog ion collectors for mass spectrometry has changed strikingly little for seventy years. Early instruments already employed much of the detector technology we recognize today, including multiple collectors, secondary electron suppressors, and electronic circuits that employed high-value resistors (resistor transimpedance amplifiers, or RTIA) to amplify small currents to measurable voltages (e.g., Nier, 1940, 1947). Between the 1950s and 1980s, as the field of isotope geochemistry shifted from home-brewed instruments to commercial ones, available noble gas mass spectrometers consolidated around a design based on the Reynolds mass spectrometer using a "Nier-type" ion source, a fixed accelerating voltage, a variable magnetic field, and a single pair of collectors consisting of an analog electron multiplier (later an ion counting multiplier) and a Faraday cup, intended to be used separately for signals of different sizes (e.g., Reynolds, 1956; Bayer et al., 1989; Renne et al., 1998; Burnard and Farley, 2000). Since around 2010, multicollection has come back into vogue as improvements in electronic noise and stability have mitigated the problems of comparing beams measured on two separate amplifiers, and the field has sought ways to minimize the uncertainty conferred by the fitting of gas evolution trends in order to calculate isotopes ratios at the time of sample inlet (e.g., Mark et al., 2009; Coble et al., 2011).

The shift toward multicollection has been accompanied by a diversification of the collector technologies available, with new ion counting multipliers built with a geometry that allows multicollector spacing, and new RTIA Faraday amplifiers employing

https://doi.org/10.5194/gchron-2020-1
Preprint. Discussion started: 7 February 2020

higher-value resistors in order to take advantage of the $\sqrt{R}$ relationship between normalized signal noise and resistance (e.g., Zhang et al., 2016). These advances are not without trade-offs, however. The use of ion counting multipliers in the detector position for large beams (^{40}Ar, for example) on some instruments allows them to measure very small samples but limits their dynamic range (Jicha et al., 2016). Instruments using high-value resistor amplifiers to achieve the same goal also suffer from a loss of dynamic range, although it is not as severe, but additionally suffer from long settling times (large Tau), baseline instability, and drift in gain calibration. Indeed, these problems have limited the use of such collectors for decades, but the cost-benefit calculation has shifted due to improving electronic stability and new techniques for dealing with the Tau-correction (Zhang et al., 2016), as well as a cultural shift in the priorities of noble gas geochemistry labs toward young, small samples and higher precision (e.g., Wijbrans et al., 2011; Jicha et al., 2012; Mark et al., 2017; Rose and Koppers, 2019).

However, the desire to measure young samples well has not displaced the need to measure old samples very precisely (Sprain et al., 2015), to measure large amounts of noble gas in ice core and water samples (Lu et al., 2014), and to measure extreme abundance ratios such as those are that are typical in ^{3}He/^{4}He analyses (Espanon et al., 2014). The ideal collector, therefore, has not just a low noise floor and high sensitivity, but also a high dynamic range, the ability to switch between low and high signals with no memory, and a stable, precisely measurable gain bias between each detector. Resistor Faraday amplifiers have a fairly restricted dynamic range, with the ability to reliably measure signals over only about five orders of magnitude. Ion counting multipliers are only able to measure small signals, and suffer from significant nonlinearity at the upper and lower ends of their useful range. Analog multipliers have a much higher dynamic range, about eight orders of magnitude, but suffer from both nonlinearity and relatively short timescale gain drift. In addition, electron multipliers wear quickly and are both expensive and vulnerable to damage from vacuum accidents and large ion beams. Faraday cups are extremely linear, quiet, resilient, and cheap to manufacture, so a technological solution that extends their useful dynamic range and sensitivity to small signals is highly desirable.

Mass spectrometers have always relied on transimpedance amplifiers, which consist of an active circuit element (usually an op-amp) that converts a small input current to a high output voltage (Figure 1). The capacitive transimpedance amplifier was developed decades ago, and was an option on such venerable devices as the Keithley 6512 Electrometer, which provided the option of feedback resistors or capacitors for current measurements. The advantage of the latter was seen as the high dynamic range, while the disadvantages were the accuracy and linearity. The new ATONA capacitive transimpedance amplifier developed by Isotopx maintains the high dynamic range (effectively unlimited for noble gas measurements) and rapid response time of the earlier feedback capacitor devices while also delivering the linearity and accuracy more traditionally associated with resistor transimpedance amplifiers. The advantages of this setup, which can accurately measure extremely low signals without sacrificing stability or the ability to measure large signals, are significant for noble gas mass spectrometry and for mass spectrometry in general.

Noble gas mass spectrometers must measure an evolving signal due to the action of the instrument itself on the sample (Figure

https://doi.org/10.5194/gchron-2020-1
Preprint. Discussion started: 7 February 2020

2). Sample abundances are typically so small that the entire sample is allowed to equilibrate with the vacuum inside the mass spectrometer at the beginning of analysis, which requires that the pumps be isolated from the vacuum chamber. Starting at this time, confounding gases will be introduced through small leaks and desorption from the walls of the vacuum chamber housing the mass spectrometer, and sample gas will be consumed by ionization in the ion source and implantation in either the collector or the walls of the vacuum chamber. Because these processes change the gas composition, and therefore both the abundances and the ratios of the noble gas isotopes being measured, noble gas geochemists typically extrapolate the evolving gas signal back to the time of sample inlet—commonly referred to as "time zero"—meaning that the analysis loses statistical power as it continues in time. The advent of multicollection means that isotope ratios could be computed directly at each time point and then themselves extrapolated to "time zero," but so far noble gas geochemists have largely used multicollection simply as a means to ensure that the maximum amount of data can be collected simultaneously for each isotope.

2 Isotopx NGX and ATONA amplifier

The Isotopx NGX is a multicollector noble gas mass spectrometer with a Nier-type ion source, a Hall Probe feedback-controlled electromagnet mass analyzer, and a customizable collector block comprising fixed Faraday cup and ion counting electron multiplier detectors. The source sensitivity is approximately 10^{-3} A/Torr, the ^{36}Ar background is approximately 2×10^{-19} moles, or 5×10^{-15} cc STP, and the rise is approximately 8×10^{-18} moles, or 2×10^{-13} cc STP ^{40}Ar per minute. The NGX at LDEO has five fixed detectors, four Faraday cups and one electron multiplier, in the appropriate configuration to simultaneously collect the five isotopes of argon typically measured for ^{40}Ar/^{39}Ar dating: ^{40}Ar, ^{39}Ar, ^{38}Ar, ^{37}Ar, and ^{36}Ar. The electron multiplier is placed at the ^{36}Ar position, where signals are typically relatively small and must be measured with high precision due to the need for an accurate ^{40}Ar/^{36}Ar ratio for initial Ar correction. We chose this configuration before the ATONA became available, and in fact we believe that an ATONA would be appropriate for ^{36}Ar measurement in many (but not all) situations.

After initial installation in late 2017 with Isotopx 10^{11} Ω and 10^{12} Ω Xact amplifiers, we installed a prototype set of ATONA amplifiers on the NGX in March 2018. The ATONA is a capacitive transimpedance amplifier, which is partially described in UK patent application GB2552232. The remaining aspects of the amplifier are protected as trade secrets. The ATONA substitutes the typical high-gain resistor of an RTIA, for which one would try to minimize the capacitance of the circuit, with a capacitor and a series of proprietary circuits that allow the rate of charge accumulation (rather than the accumulated charge itself) to be continuously sampled (again, the exact mechanism used is a trade secret). The result is that the ATONA can measure a wide range of ion beam currents, from attoamps to nanoamps (hence the name), with good linearity, very low noise, and a settling time short enough to be insignificant (less than the 2 ms sampling time of the measurement electronics).

The ATONA has the important characteristic that the noise scales inversely with time, rather than with the square root of time, so accumulating a signal for longer between sampling intervals will result in a linearly less noisy signal. Counting statistics reduces uncertainty with the square root of time, so by comparison the ATONA gains an additional factor of the square root

https://doi.org/10.5194/gchron-2020-1
Preprint. Discussion started: 7 February 2020

of time in noise reduction when the sampling interval is extended. There is a trade-off in noble gas mass spectrometry because of the evolution of the signal with time, although it is important to mention that the signal from the production version of the ATONA can be subsampled without sacrificing the gain of the longer sampling time. This dynamic opens up a wide array of possibilities of best measurement practice that will vary with ion beam size, and we have not yet fully explored them. The work presented here has led us to settle on an integration time of 10 seconds, with a typical total analysis time of 600 seconds in multicollection mode, as a sweet spot for reducing noise without sacrificing gas evolution fit statistics. Analytical conditions for different experiments in this study vary and are described in the figure captions. All isotope evolutions are fit using a linear regression with no outlier data points excluded from either fits or uncertainty calculations, and with no measurement cycles discarded from the analysis. The only exception is in Section 3.3, in which we removed the final 200 seconds from a set of 600-second APIS analyses in order to allow a direct comparison to a dataset of 400-second analyses on a different mass spectrometer.

3 Analyses of electronics and gas standards

3.1 Background noise

Reported detector signal units are an arbitrary choice in mass spectrometry; the important quantity for a given detector is signal/noise ratio produced by a given incident ion beam. We quantify this by converting measured signal from detector units to incident ion beam current using Ohm's Law for voltage measured on an RTIA. The ATONA does not measure voltage in the same way as an RTIA, but its firmware converts the signal to equivalent 10^{11} Ω RTIA volts. We convert back to beam current for clearer comparison with RTIAs that have a different gain, and with other types of detectors. As an example, 1 10^{11} Ω RTIA volt is equivalent to 10^4 fA, and 625 cps on an ion counting electron multiplier is equivalent to 0.1 fA. We calculate background noise for ideal RTIAs with a variety of feedback resistors. In this case, we assume that the only significant component of noise is Johnson–Nyquist noise, or thermal white noise, which provides an absolute limit for the signal/noise ratio achievable with an RTIA. The best commercial RTIAs approach this limit.

Unlike Johnson noise, kTC noise (capacitor thermal noise, equal to the product of the Boltzmann constant, k, and the absolute temperature, T, divided by the capacitance, C) has no frequency component. This means that the voltage noise produced by a current discharged from a capacitor will scale linearly with time. As a result, one might expect to achieve a factor of $1/\sqrt{t}$ in noise reduction by extending the charge accumulation time arbitrarily. This is not exactly how the ATONA functions, as one is able to subsample the measurement without losing the benefit of a longer integration time, but the expected linear relationship is achieved. The theoretical noise floor of the ATONA design is not immediately apparent from the publicly-available information about its capabilities, which do not reveal either the design of the measurement circuit or the value of the capacitor employed. A simple calculation assuming kTC noise is the only source of noise on each ATONA measurement yields a value of 15-20 pF for the complete circuit, which includes both the capacitor used on the amplifier and the capacitance of the Faraday collectors themselves and the wires and feedthroughs that connect them. We measure noise directly through a series

https://doi.org/10.5194/gchron-2020-1
Preprint. Discussion started: 7 February 2020

of measurements on the Isotopx NGX with the instrument under vacuum, all lenses active, and the filament powered off. We then express this noise floor in terms of incident ion beam for direct comparison to RTIAs.

The results are plotted in two different ways. First, we show a series of measurements of ATONA noise compared to ideal RTIA Johnson noise calculations for a series of RTIA resistor values in Figure 3. This figure simply shows measurements taken with the ATONA with no ion beam, with the arithmetic mean of the measurements subtracted from each. This is, therefore, what a series of measurements of a stable beam would look like to the user during a measurement cycle. Each measurement is made with a ten second integration, which is the typical integration time we use for the ATONA on most samples. The ATONA measurements have a standard deviation of 0.0085 fA, which is equivalent to 0.85 μV on a 10^{11} RTIA. In Figure 4, we show the same noise data as 1-σ standard deviation of a signal plotted as a function of integration time to show the different behavior of the ATONA as integration time is changed. Using a one second or 100 second integration time, the ATONA measurements have standard deviations of 0.073 fA and 0.0018 fA, respectively. The ten-second integration time value compares favorably to a 10^{13} RTIA at 0.011 fA, but does not quite reach the low noise level of a 10^{14} RTIA at 0.0040 fA. Similarly, at one second integration, the ATONA is in between the 10^{12} and 10^{13} RTIA (0.40 fA, 0.037 fA, respectively).

3.2 Air standards

We prepared a large air standard of approximately 8.5×10^{-13} moles of Ar for mass spectrometer installation and initial testing. We used air taken at a distance from the Lamont-Doherty Earth Observatory Comer geochemistry building in Palisades, NY, on a dry day in November, and we filled the approximately six liter standard tank with one aliquot from the approximately 0.1 cc pipette. Subsequent aliquots for measurement were taken from the standard tank using the same pipette, attached to a custom-built high vacuum system containing a hot SAES St101 getter. The size of the resulting Ar aliquot introduced to the mass spectrometer was estimated first from the approximate volumes of the standard tank, pipette, and vacuum system, then refined by comparison to the GLO glauconite argon concentration standard and by comparison to a standard tank on another mass spectrometer with a manometrically calibrated volume.

We measured four different splits of the air standard ranging from the full aliquot to approximately 0.36% of the total. The split sizes of 100%, 17.7%, and 2.6% are most useful for comparing the Isotopx Xact RTIA to the ATONA. For all Xact measurements, a 10^{11} Ω amplifier was used for ^{40}Ar and a 10^{12} Ω amplifier was used for ^{38}Ar. The ATONA amplifiers all use the same feedback capacitor and are therefore interchangeable. The ^{40}Ar/^{38}Ar ratios for these standards, which provide a direct comparison of the performance of the amplifiers without the effect of the ion counting multiplier used to measure ^{36}Ar, are shown in Figure 5. For the different shot sizes, the Xact amplifiers produced standard deviations of 0.43%, 3.07%, and 27.9%, respectively, while the ATONA amplifiers produced standards deviations of 0.21%, 1.35%, and 7.87%. As predicted based on zero-beam noise measurements, the ATONA outperforms the Xact for all signal sizes. The improvement between the Xact and the ATONA is greater for smaller beam sizes because the effect of amplifier Johnson noise on the total uncertainty comes to dominate over other factors like source instability when the signal is smaller.

https://doi.org/10.5194/gchron-2020-1
Preprint. Discussion started: 7 February 2020

In order to provide a more rigorous assessment of the ATONA amplifiers themselves and to produce an amplifier-only dataset for $^{40}Ar/^{36}Ar$, which is a more commonly discussed isotope ratio in $^{40}Ar/^{39}Ar$ geochronology, we then switched to single collector mode. Using the ATONA amplifiers, we measured each species by peak-hopping on the H2 collector, which is normally used for ^{40}Ar, and we measured $^{40}Ar/^{38}Ar$ and $^{40}Ar/^{36}Ar$ for splits of our air standard ranging from 200% (representing two aliquots of the full standard) to 0.36%, representing three splits with the extraction line, or approximately 3×10^{-15} moles of Ar. The $^{40}Ar/^{36}Ar$ ratios for these measurements are shown in Figure 6, and the $^{40}Ar/^{38}Ar$ ratios are shown in Figure A1. The measured ratios along with internal uncertainties and standard deviations between analyses are shown in Table 1 for $^{40}Ar/^{36}Ar$, and in Table A1 for $^{40}Ar/^{38}Ar$.

Finally, we measured the same ion beam (^{40}Ar) repeatedly on each Faraday detector to determine the gain bias between the different ATONA amplifiers. Choosing the axial detector as a reference, the relative gains of the other detectors ranged was between 1.6 and 3.6 ‰ lower, with a standard deviation of between 106 and 220 ppm for the intercalibration factor of each detector when measured using 1-second integration periods for 10 periods of 10 seconds on each detector (Figure A2). Because we used a real Ar beam measured with a sequential peak hop rather than a synthetically produced calibration voltage, fluctuations in the ion source and mass analyzer electronics might also contribute noise to these measurements, so this is a maximum estimate of the intercalibration drift of the ATONA. The production model of the ATONA amplifiers, which are now being installed on some TIMS instruments, have a calibration voltage that eliminates these other sources of uncertainty; preliminary results from this system show a standard deviation of only 0.6 ppm for each detector when measured using two-minute integration periods over multiple four hour blocks (Szymanowski and Schoene, 2019).

Because the uncertainty of the measured signals is dominated by the thermal noise of the Faraday amplifier, the uncertainty of each measured ratio is controlled largely by the uncertainty of the smaller isotope. For comparison to other instruments, we plot each measured isotope ratio as a function of the sample size of the small isotope in the ratio in Figure 7 (that is, for the same air standard, the $^{40}Ar/^{36}Ar$ ratio will plot approximately five times higher in terms of sample size than the $^{40}Ar/^{38}Ar$ ratio, because the $^{40}Ar/^{36}Ar$ ratio of air is 298.56 while the $^{40}Ar/^{38}Ar$ ratio of air is 1583.87 (Lee et al., 2006; Mark et al., 2011). This reference frame allows us to compare unlike detectors such as analog multipliers and Faraday cups, as well as to compare isotope ratios measured using a mix of detector types, such as the $^{40}Ar/^{36}Ar$ ratios measured in the standard multicollection mode of our NGX. While a better reference frame for direct comparison of detector technologies might be beam size rather than sample size, the latter choice allows for a more realistic comparison of mass spectrometers as they are used in the laboratory. We also note that while most noble gas mass spectrometers provide a similar specification for constant pressure ion source sensitivity, field reports indicate that some (notably the Thermo Argus) have an advantage due to both smaller volume and higher constant pressure sensitivity. These results show a clear improvement for the NGX with ATONA compared to the previous generation of mass spectrometer (represented by the LDEO VG 5400) and the NGX with XAct 10^{12} Ω RTIA (the same NGX at LDEO, with its original amplifiers). The performance is also better than published data for the Thermo Argus

https://doi.org/10.5194/gchron-2020-1
Preprint. Discussion started: 7 February 2020

with 10^{12} Ω RTIA (Mark et al., 2009), despite the Argus' apparently higher source sensitivity, which is consistent with the prediction that the ATONA will easily outperform a 10^{12} Ω RTIA (Figure 3); see Section 3.3 for a comparison to the Argus with a 10^{13} Ω RTIA. Finally, the NGX using its ion counting multiplier in peak-hopping mode is still able to achieve a much lower noise level for very small samples, comparable to the Nu Noblesse with multiple ion counting multipliers (Jicha et al., 2016), which is also consistent with the predicted noise level of the ATONA. However, these detectors are limited to very small samples; the data points with more than 10^{-17} moles of ^{36}Ar in Figure 7 actually use an ATONA for the ^{40}Ar beam, but we plot them in the ICM category because the uncertainty of the small isotope controls the uncertainty of the ratio measurement.

3.3 APIS cocktail standards

The Argon Intercalibration Pipette System (APIS) is a system designed to provide a portable set of argon gas standards of different size and isotope ratio for a noble gas mass spectrometer (Turrin et al., 2015). The APIS has three standard tanks containing air, a cocktail representing argon with a ^{40}Ar/^{39}Ar ratio typical of an irradiated Alder Creek sanidine standard, and a cocktail representing argon with a ^{40}Ar/^{39}Ar ratio typical of an irradiated Fish Canyon Tuff sanidine standard. Each tank has three pipettes attached to it, with volumes of 0.1, 0.2, and 0.4 cc, allowing aliquots of gas ranging in size from 1 to 7 times the size of the 0.1 cc pipette to be extracted without resorting to multiple aliquots from a single pipette. We measured each possible size, 0.1 cc, 0.2 cc, 0.3 cc, 0.4 cc, 0.5 cc, 0.6 cc, and 0.7 cc, three times from each of the Alder Creek and Fish Canyon Tuff tanks, and six times from the air standard, interspersed with our lab standard and procedural blanks.

The APIS standards have accumulated air background since the system was first deployed, so a direct comparison of measured ratios is not possible. However, we can compare air-corrected values for the Fish Canyon and Alder Creek standard tanks—similar to what would be measured during an actual experiment. As an example, we plot measured radiogenic ^{40}Ar*/^{39}Ar values (^{40}Ar/^{39}Ar ratios corrected for air contamination using simultaneously measured ^{40}Ar*/^{36}Ar ratios) for the Fish Canyon analog from the Isotopx NGX with the ATONA (10-second integration periods; 400 seconds measurement time) and the Thermo Argus with the 10^{12} Ω and 10^{13} Ω RTIA (1-second integration periods; 400 seconds measurement time; Figure 8; Ross and Mcintosh, 2016). While the ATONA exhibits lower noise on a per-signal basis, the higher sensitivity of the Argus ion source makes the results indistinguishable.

4 Summary

The ATONA amplifier represents a significant step forward in Faraday cup amplifier technology for noble gas mass spectrometry. The ATONA allows a greater dynamic range of ion beams to be measured compared to existing RTIA technology, and only highly specialized RTIA electronics are able to compete with the low noise of the ATONA. The noise and gain bias of the amplifiers are significantly more stable than both RTIAs and electron multipliers. Other types of mass spectrometer that produce a stable ion beam are likely to see an even greater performance improvement with the ATONA because of its ability to capitalize on long integration times to reduce noise. The strengths of the ATONA, combining low noise for small samples

https://doi.org/10.5194/gchron-2020-1
Preprint. Discussion started: 7 February 2020

with high dynamic range and good stability for large samples, are in harmony with the current priorities of the field of noble gas geochemistry, which require instruments that can deliver both high precision and flexibility for measuring a wide range of sample types.

Author contributions. SEC installed the instrument, set up hardware and software, designed experiments, performed measurements, and interpreted the results. SRH designed experiments, performed measurements, and interpreted results. DT designed and implemented the ATONA system and installed the prototype on the NGX at LDEO.

Competing interests. DT is an employee of Isotopx, Ltd.

Acknowledgements. We thank Jake Ross for extensive discussion and Pychron programming help and for sharing raw data from NMGRL measurements published in conference proceedings and Brian Jicha for discussion and for sharing raw data from WiscAr mesaurements published in *Chemical Geology*. We also thank Chris Varden for initial installation and testing of the NGX at LDEO.

https://doi.org/10.5194/gchron-2020-1
Preprint. Discussion started: 7 February 2020

References

Bayer, R., Schlosser, P., Bönisch, G., Rupp, H., Zaucker, F., and Zimmek, G.: Performance and Blank Components of a Mass Spectrometric System for Routine Measurement of Helium Isotopes and Tritium by the 3He Ingrowth Method, Springer Berlin Heidelberg, Berlin, Heidelberg, https://doi.org/10.1007/978-3-642-48373-8, http://link.springer.com/10.1007/978-3-642-48373-8, 1989.

Burnard, P. G. and Farley, K. A.: Calibration of pressure-dependent sensitivity and discrimination in Nier-type noble gas ion sources: TECHNICAL BRIEF, Geochemistry, Geophysics, Geosystems, 1, n/a–n/a, https://doi.org/10.1029/2000GC000038, http://doi.wiley.com/10.1029/2000GC000038, 2000.

Coble, M. A., Grove, M., and Calvert, A. T.: Calibration of Nu-Instruments Noblesse multicollector mass spectrometers for argon isotopic measurements using a newly developed reference gas, Chemical Geology, 290, 75–87, https://doi.org/10.1016/j.chemgeo.2011.09.003, https://linkinghub.elsevier.com/retrieve/pii/S0009254111003524, 2011.

Espanon, V. R., Honda, M., and Chivas, A. R.: Cosmogenic 3He and 21Ne surface exposure dating of young basalts from Southern Mendoza, Argentina, Quaternary Geochronology, 19, 76–86, https://doi.org/10.1016/j.quageo.2013.09.002, https://linkinghub.elsevier.com/retrieve/pii/S1871101413000769, 2014.

Jicha, B. R., Rhodes, J. M., Singer, B. S., and Garcia, M. O.: 40Ar/39Ar geochronology of submarine Mauna Loa volcano, Hawaii, Journal of Geophysical Research: Solid Earth, 117, https://doi.org/10.1029/2012JB009373, http://doi.wiley.com/10.1029/2012JB009373, 2012.

Jicha, B. R., Singer, B. S., and Sobol, P.: Re-evaluation of the ages of 40Ar/39Ar sanidine standards and supereruptions in the western U.S. using a Noblesse multi-collector mass spectrometer, Chemical Geology, 431, 54–66, https://doi.org/10.1016/j.chemgeo.2016.03.024, https://linkinghub.elsevier.com/retrieve/pii/S0009254116301474, 2016.

Lee, J.-Y., Marti, K., Severinghaus, J. P., Kawamura, K., Yoo, H.-S., Lee, J. B., and Kim, J. S.: A redetermination of the isotopic abundances of atmospheric Ar, Geochimica et Cosmochimica Acta, 70, 4507–4512, https://doi.org/10.1016/j.gca.2006.06.1563, https://linkinghub.elsevier.com/retrieve/pii/S0016703706018679, 2006.

Lu, Z.-T., Schlosser, P., Smethie, W., Sturchio, N., Fischer, T., Kennedy, B., Purtschert, R., Severinghaus, J., Solomon, D., Tanhua, T., and Yokochi, R.: Tracer applications of noble gas radionuclides in the geosciences, Earth-Science Reviews, 138, 196–214, https://doi.org/10.1016/j.earscirev.2013.09.002, https://linkinghub.elsevier.com/retrieve/pii/S0012825213001517, 2014.

Mark, D., Stuart, F., and de Podesta, M.: New high-precision measurements of the isotopic composition of atmospheric argon, Geochimica et Cosmochimica Acta, 75, 7494–7501, https://doi.org/10.1016/j.gca.2011.09.042, https://linkinghub.elsevier.com/retrieve/pii/S0016703711005631, 2011.

Mark, D. F., Barfod, D., Stuart, F. M., and Imlach, J.: The ARGUS multicollector noble gas mass spectrometer: Performance for 40Ar/39Ar geochronology, Geochemistry, Geophysics, Geosystems, 10, n/a–n/a, https://doi.org/10.1029/2009GC002643, http://doi.wiley.com/10.1029/2009GC002643, 2009.

Mark, D. F., Renne, P. R., Dymock, R. C., Smith, V. C., Simon, J. I., Morgan, L. E., Staff, R. A., Ellis, B. S., and Pearce, N. J.: High-precision 40Ar/39Ar dating of pleistocene tuffs and temporal anchoring of the Matuyama-Brunhes boundary, Quaternary Geochronology, 39, 1–23, https://doi.org/10.1016/j.quageo.2017.01.002, https://linkinghub.elsevier.com/retrieve/pii/S1871101417300055, 2017.

Nier, A. O.: A Mass Spectrometer for Routine Isotope Abundance Measurements, Review of Scientific Instruments, 11, 212–216, https://doi.org/10.1063/1.1751688, http://aip.scitation.org/doi/10.1063/1.1751688, 1940.

Nier, A. O.: A Mass Spectrometer for Isotope and Gas Analysis, Review of Scientific Instruments, 18, 398–411, https://doi.org/10.1063/1.1740961, http://aip.scitation.org/doi/10.1063/1.1740961, 1947.

https://doi.org/10.5194/gchron-2020-1
Preprint. Discussion started: 7 February 2020

Renne, P. R., Swisher, C. C., Deino, A. L., Karner, D. B., Owens, T. L., and DePaolo, D. J.: Intercalibration of standards, absolute ages and uncertainties in 40Ar/39Ar dating, Chemical Geology, 145, 117–152, https://doi.org/10.1016/S0009-2541(97)00159-9, https://linkinghub.elsevier.com/retrieve/pii/S0009254197001599, 1998.

Reynolds, J. H.: High Sensitivity Mass Spectrometer for Noble Gas Analysis, Review of Scientific Instruments, 27, 928–934, https://doi.org/10.1063/1.1715415, http://aip.scitation.org/doi/10.1063/1.1715415, 1956.

Rose, J. and Koppers, A. A.: Simplifying Age Progressions within the Cook-Austral Islands using ARGUS-VI High-Resolution ^{40} Ar/ ^{39} Ar Incremental Heating Ages, Geochemistry, Geophysics, Geosystems, 20, 4756–4778, https://doi.org/10.1029/2019GC008302, https://onlinelibrary.wiley.com/doi/abs/10.1029/2019GC008302, 2019.

Ross, J. and Mcintosh, W.: Pychron: Everything you didn't know you wanted in a geochronology application, in: Geological Society of America Abstracts with Programs, vol. 48, The Geological Society of America, Denver, CO, https://doi.org/10.1130/abs/2016AM-286732, 2016.

Sprain, C. J., Renne, P. R., Wilson, G. P., and Clemens, W. A.: High-resolution chronostratigraphy of the terrestrial Cretaceous-Paleogene transition and recovery interval in the Hell Creek region, Montana, Geological Society of America Bulletin, 127, 393–409, https://doi.org/10.1130/B31076.1, https://pubs.geoscienceworld.org/gsabulletin/article/127/3-4/393-409/126101, 2015.

Szymanowski, D. and Schoene, B.: U–Pb TIMS Geochronology Using ATONA Amplifiers [V11D-0124], in: AGU Fall Meeting 2019, AGU, San Francisco, CA, 2019.

Turrin, B. D., Swisher, III, C. C., Hemming, S. R., Renne, P. R., Deino, A. L., Hodges, K. V., Van Soest, M. C., and Heizler, M. T.: An Update to the EARTHTIME Argon Intercalibration Pipette System (APIS): Smoking from the Same Pipe, in: AGU, Fall Meeting 2015, pp. V53H–08, AGU, San Francisco, CA, https://agu.confex.com/agu/fm15/meetingapp.cgi/Paper/84132, 2015.

Wijbrans, J., Schneider, B., Kuiper, K., Calvari, S., Branca, S., De Beni, E., Norini, G., Corsaro, R. A., and Miraglia, L.: 40Ar/39Ar geochronology of Holocene basalts; examples from Stromboli, Italy, Quaternary Geochronology, 6, 223–232, https://doi.org/10.1016/j.quageo.2010.10.003, https://linkinghub.elsevier.com/retrieve/pii/S1871101410000658, 2011.

Zhang, X., Honda, M., and Hamilton, D.: Performance of the High Resolution, Multi-collector Helix MC Plus Noble Gas Mass Spectrometer at the Australian National University, Journal of The American Society for Mass Spectrometry, 27, 1937–1943, https://doi.org/10.1007/s13361-016-1480-3, http://link.springer.com/10.1007/s13361-016-1480-3, 2016.

https://doi.org/10.5194/gchron-2020-1
Preprint. Discussion started: 7 February 2020

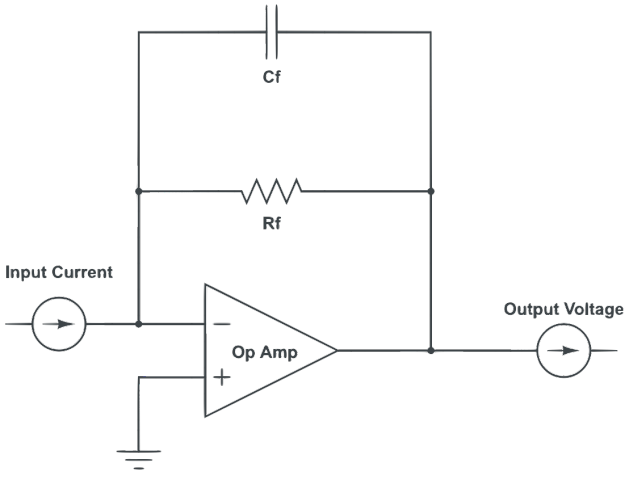

Figure 1. Schematic of a transimpedance amplifier. Note that practical examples are far more complex. The circuit consists of an op-amp, which is the active element that converts the input current to a proportional output voltage, and then a feedback resistor and capacitor that determine the gain of the circuit. In a traditional resistance transimpedance amplifier, the resistor is very high value and the capacitance is reduced as much as is practical. The ATONA instead uses a defined capacitance as the feedback element.

https://doi.org/10.5194/gchron-2020-1
Preprint. Discussion started: 7 February 2020

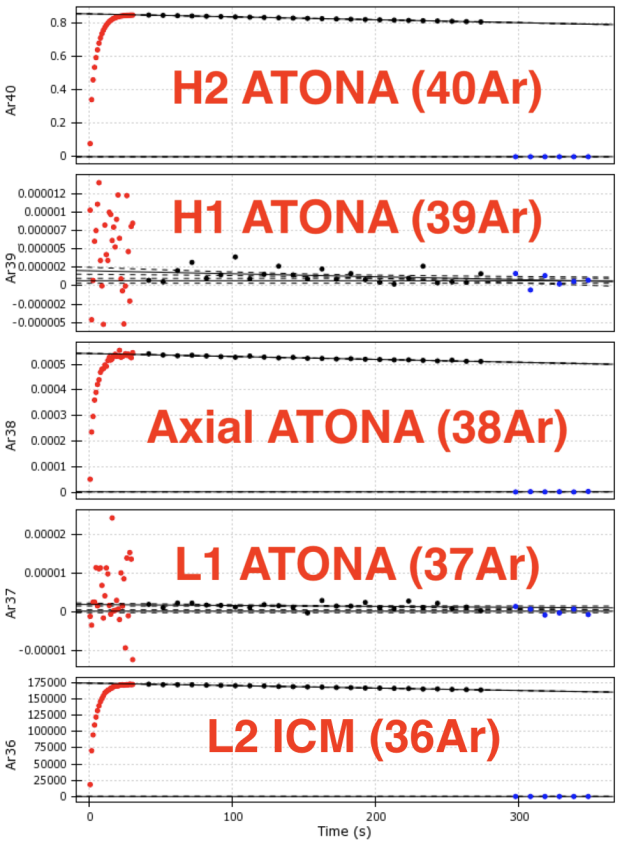

Figure 2. An example measurement of the 8.5×10^{-13} mole Ar air standard on the Isotopx NGX. The gas is measured with a one-second integration time during 30 seconds of sample inlet, then with a ten-second integration time during 240 seconds of measurement and 60 seconds of baseline measurement. The figure shows the live measurement screen displayed in Pychron during automated sample analysis with overlain labels. Each signal is displayed as reported by the Isotopx software: volts for the four Faraday collectors (converted by the onboard ATONA firmware to equivalent 10^{11} Ω RTIA volts) and counts per second for the ion counting electron multiplier.

https://doi.org/10.5194/gchron-2020-1
Preprint. Discussion started: 7 February 2020

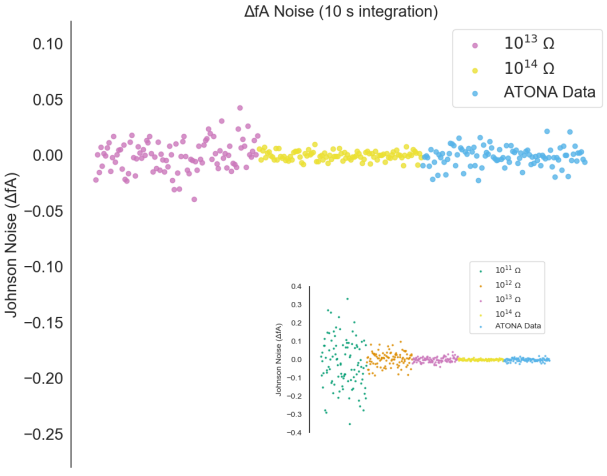

Figure 3. Measured noise on the ATONA amplifiers expressed as deviations from the average signal with no ion beam in the mass spectrometer compared to ideal 10^{13} Ω and 10^{14} Ω RTIA noise. The signals are converted to equivalent ion beam current (see Section 3.1. Each measurement and ideal RTIA calculation is made over ten seconds of integration and then simply plotted in order. The inset includes 10^{11} Ω and 10^{12} Ω examples as well, with the same ATONA data. Examples using 1-second and 100-second integration times are included in the appendix.

https://doi.org/10.5194/gchron-2020-1
Preprint. Discussion started: 7 February 2020

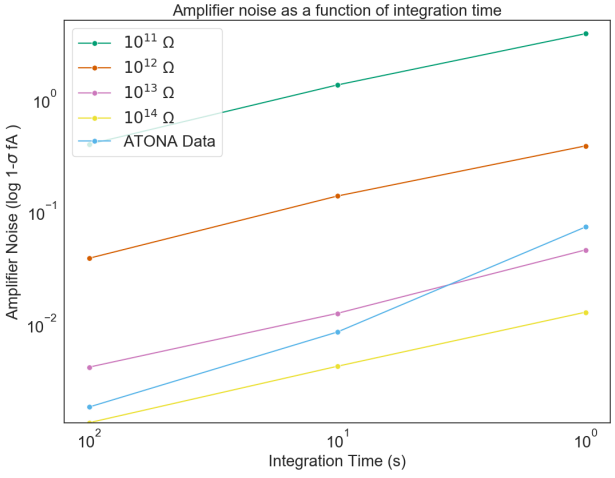

Figure 4. Noise expressed as standard deviation of signal measured (ATONA) or calculated (ideal RTIA) for the ATONA and 10^{11} Ω, 10^{12} Ω, 10^{13} Ω, and 10^{14} Ω RTIA. The ATONA noise decreases more quickly with increasing integration time because of the $1/t$ (rather than $1/\sqrt{t}$) relationship between noise and integration time.

https://doi.org/10.5194/gchron-2020-1
Preprint. Discussion started: 7 February 2020

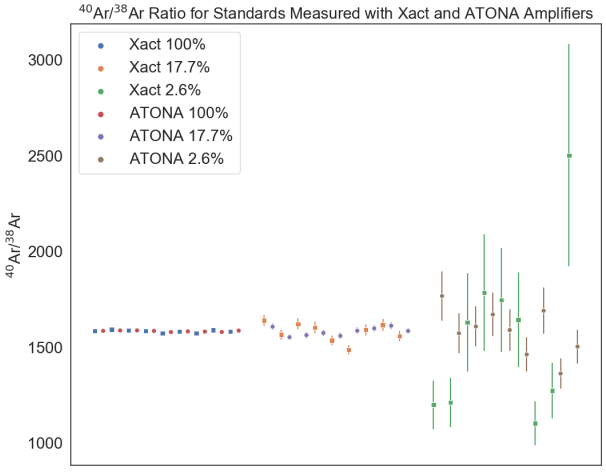

Figure 5. $^{40}Ar/^{38}Ar$ ratios for air standard splits of 100%, 17.7%, and 2.6% measured using both the Isotopx Xact (10^{11} Ω for ^{40}Ar and 10^{12} Ω for ^{38}Ar) amplifiers and the ATONA amplifiers in multicollection mode. Each sequence shows nine air standards measured sequentially, interspersed with blanks, for 600 seconds each. The ATONA measurements and the Xact measurements were both made using 600 1-second integration periods; ATONA performance improves even further with longer integration periods.

https://doi.org/10.5194/gchron-2020-1
Preprint. Discussion started: 7 February 2020

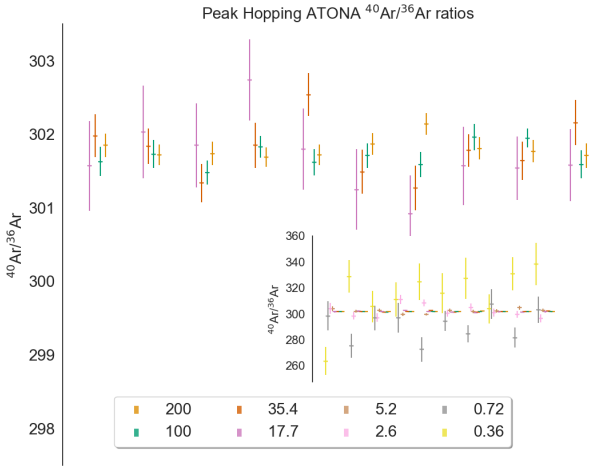

Figure 6. $^{40}Ar/^{36}Ar$ ratios for air standard splits between 200% and 17.7% (inset: 200% and 0.36%) measured using the Isotopx ATONA amplifiers in single collector peak-hopping mode, with the ^{36}Ar, ^{38}Ar, and ^{40}Ar beams measured in sequence on the H2 Faraday. Each beam was measured in sets of three 10-second integration periods, which repeated ten times. Each sequence shows ten air standards, plotted interspersed for comparison.

https://doi.org/10.5194/gchron-2020-1
Preprint. Discussion started: 7 February 2020

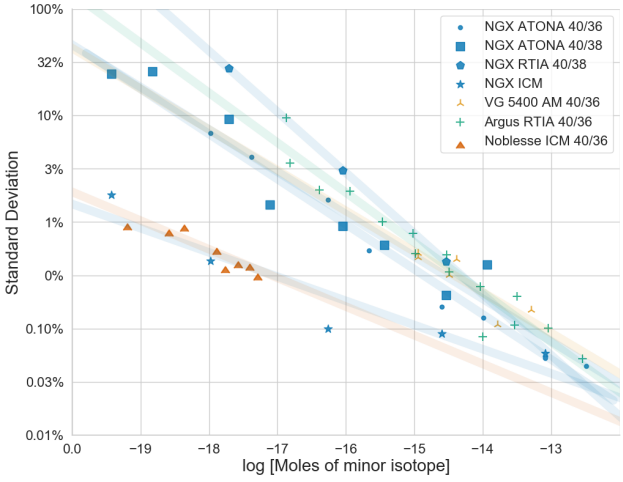

Figure 7. Standard deviation of measured ^{40}Ar/^{36}Ar or ^{40}Ar/^{38}Ar ratios for air standards measured on different mass spectrometers as a function of small isotope abundance in moles. ATONA is the ATONA amplifier described here, RTIA is a traditional resistor transimpedance Faraday amplifier, ICM is an ion counting multiplier, and AM is an analog multiplier. The NGX data points with more than 10^{-17} moles of ^{36}Ar use an ATONA for the ^{40}Ar beam, but in all cases the uncertainty of the small isotope controls the uncertainty of the ratio. This plot provides a direct comparison of whole instrument performance rather than detector performance because the ion source and mass analyzer also contribute to uncertainty in the measurements, and the sample abundance is not weighted by source sensitivity. We note that we are not able to completely control for the effects of different analytical conditions, including background, detector integration time, total measurement time, sensitivity, and data reduction.

https://doi.org/10.5194/gchron-2020-1
Preprint. Discussion started: 7 February 2020

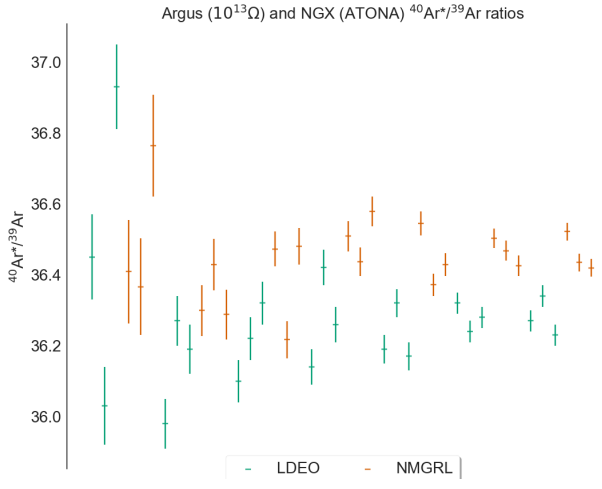

Figure 8. Air-corrected ^{40*}Ar/^{39}Ar ratios for the APIS Fish Canyon Tuff analog standard on the Isotopx NGX with the ATONA at Lamont-Doherty Earth Observatory and the Thermo Argus with the 10^{12} Ω and 10^{13} Ω RTIA at the New Mexico Geochronology Research Laboratory (Ross and Mcintosh, 2016), with smaller (0.1 cc) aliquots on the left, and 0.2, 0.3, 0.4, 0.5, 0.6, and 0.7 cc aliquots to the right. Both sets of measurements were performed with 400 seconds of analysis time in multicollection. The ATONA data were collected using 10-second integration periods, while the Argus data were collected using 1-second integration periods. The standard deviation of the signals for a given size aliquot is comparable for the two instruments.

https://doi.org/10.5194/gchron-2020-1
Preprint. Discussion started: 7 February 2020

Table 1. $^{40}Ar/^{36}Ar$ of air standards measured in peak-hopping mode on a single ATONA Faraday cup on the LDEO NGX. Standards were measured using ten cycles each of three ten-second integration periods for each isotope, in the order ^{36}Ar, ^{38}Ar, ^{40}Ar.

Split Size	200%		100%		35.4%		17.7%		5.2%		2.6%		0.72%		0.36%	
Moles	1.7E-12		8.5E-13		3.0E-13		1.5E-13		4.4E-14		2.2E-14		6.1E-15		3.1E-15	
	$^{40}Ar/^{36}Ar$	±	$^{40}Ar/^{36}Ar$	±	$^{40}Ar/^{36}Ar$	±	$^{40}Ar/^{36}Ar$	±	$^{40}Ar/^{36}Ar$	±	$^{40}Ar/^{36}Ar$	±	$^{40}Ar/^{36}Ar$	±	$^{40}Ar/^{36}Ar$	±
	301.85	0.16	301.63	0.2	301.98	0.29	301.57	0.61	303.95	1.95	304.18	4.07	298.44	11.21	263.6	10.83
	301.72	0.14	301.73	0.19	301.84	0.24	302.03	0.63	301.91	1.17	298.3	2.88	275.24	9.29	328.75	12.51
	301.74	0.16	301.48	0.16	301.34	0.26	301.85	0.57	302.75	1.39	297.1	3.14	296.75	9.44	305.53	11.93
	301.69	0.13	301.83	0.15	301.85	0.31	302.74	0.55	299.69	1.31	310.96	3.49	296.99	11.28	311.06	13.04
	301.72	0.14	301.62	0.18	302.54	0.29	301.8	0.55	299.5	0.99	308.39	2.59	272.54	9.51	324.64	14.03
	301.87	0.15	301.71	0.17	301.49	0.3	301.25	0.55	302.6	1.32	300.24	2.4	294.46	7.82	315.81	15.25
	302.14	0.15	301.59	0.17	301.27	0.3	300.92	0.52	301.75	1.21	304.97	3.17	284.62	6.65	327.28	15.75
	301.81	0.15	301.96	0.18	301.78	0.22	301.57	0.53	302.38	1.29	300.98	3.18	307.42	11.47	303.86	11.31
	301.77	0.15	301.95	0.13	301.64	0.26	301.54	0.43	304.76	1.52	299.41	2.62	281.71	7.78	330.93	12.68
	301.71	0.17	301.59	0.19	302.16	0.31	301.58	0.49	302.64	1.41	296.59	3.09	303.07	9.99	338.41	16.31
1-σ	0.13		0.16		0.38		0.48		1.6		4.9		12		21	
1-σ (%)	0.044%		0.053%		0.13%		0.16%		0.54%		1.6%		4.1%		6.8%	

https://doi.org/10.5194/gchron-2020-1
Preprint. Discussion started: 7 February 2020

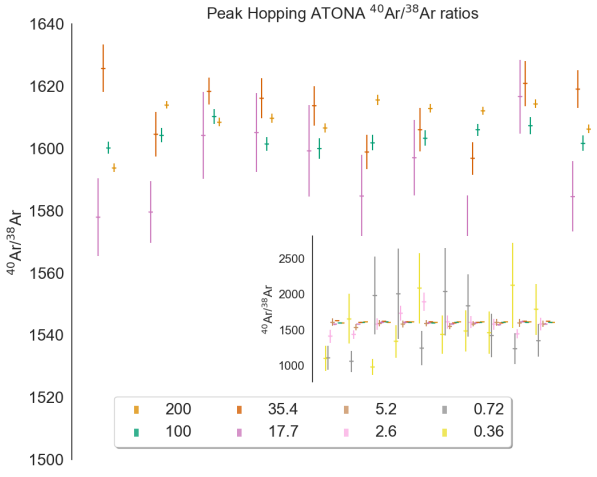

Figure A1. $^{40}Ar/^{38}Ar$ ratios for air standard splits between 200% and 17.7% (inset: 200% and 0.36%) measured using the Isotopx ATONA amplifiers in single collector peak-hopping mode, with the ^{36}Ar, ^{38}Ar, and ^{40}Ar beams measured in sequence on the H2 Faraday. Each beam was measured in sets of three 10-second integration periods, which repeated ten times. Each sequence shows ten air standards, plotted interspersed for comparison.

https://doi.org/10.5194/gchron-2020-1
Preprint. Discussion started: 7 February 2020

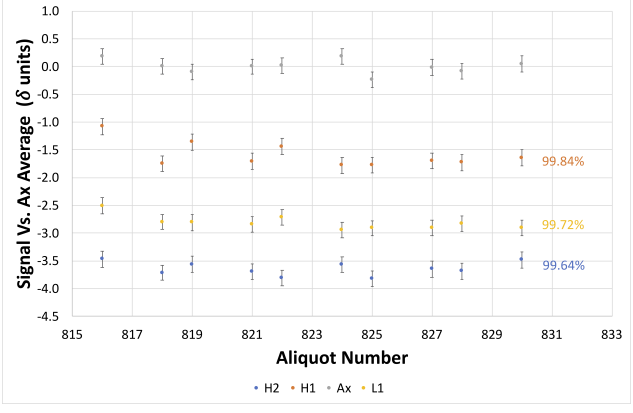

Figure A2. Intercalibration measurements using an ^{40}Ar beam produced by aliquots of the air standard, measured by peak hopping just the ^{40}Ar beam on each of the four ATONA Faraday collectors on the NGX. Measurements were made using sets of ten 1-second integration periods, repeated ten times sequentially on each detector. The detector intercalibration factor ranges from 0.9964 to 0.9984 for the other three detectors relative to the axial detector, with standard deviations ranging from 106 to 220 ppm for each.

https://doi.org/10.5194/gchron-2020-1
Preprint. Discussion started: 7 February 2020

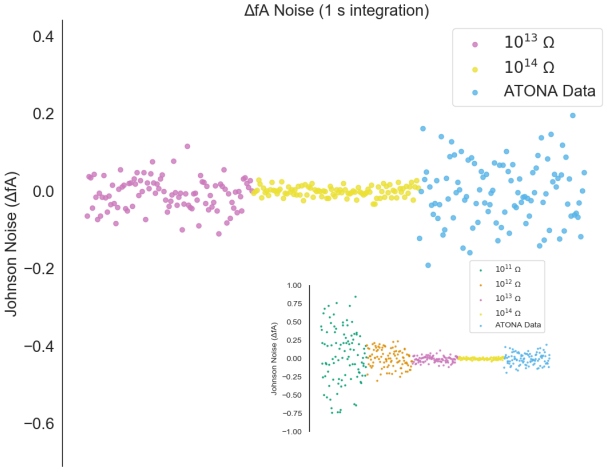

Figure A3. Measured noise on the ATONA amplifiers expressed as deviations from the average signal with no ion beam in the mass spectrometer compared to ideal 10^{13} Ω and 10^{14} Ω RTIA noise. The signals are converted to equivalent ion beam current (see Section 3.1. Each measurement and ideal RTIA calculation is made over one second of integration and then simply plotted in order. The inset includes 10^{11} Ω and 10^{12} Ω examples as well, with the same ATONA data. Examples using a 10-second integration times are included in Figure 3.

https://doi.org/10.5194/gchron-2020-1
Preprint. Discussion started: 7 February 2020

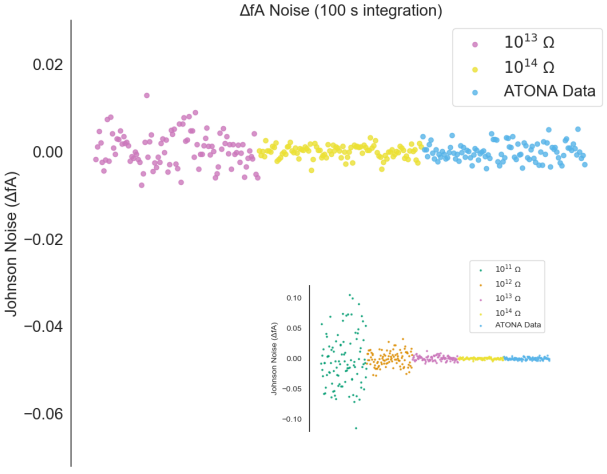

Figure A4. Measured noise on the ATONA amplifiers expressed as deviations from the average signal with no ion beam in the mass spectrometer compared to ideal 10^{13} Ω and 10^{14} Ω RTIA noise. The signals are converted to equivalent ion beam current (see Section 3.1. Each measurement and ideal RTIA calculation is made over 100 seconds of integration and then simply plotted in order. The inset includes 10^{11} Ω and 10^{12} Ω examples as well, with the same ATONA data. Examples using a 10-second integration times are included in Figure 3.

https://doi.org/10.5194/gchron-2020-1
Preprint. Discussion started: 7 February 2020

GEOCHRONOLOGY Discussions Open Access EGU

Table A1. $^{40}Ar/^{38}Ar$ of air standards measured in peak-hopping mode on a single ATONA Farday cup.

Split Size	200%		100%		35.4%		17.7%		5.2%		2.6%		0.72%		0.36%	
Moles	1.7E-12		8.5E-13		3.0E-13		1.5E-13		4.4E-14		2.2E-14		6.1E-15		3.1E-15	
	$^{40}Ar/^{38}Ar$	±	$^{40}Ar/^{38}Ar$	±	$^{40}Ar/^{38}Ar$	±	$^{40}Ar/^{38}Ar$	±	$^{40}Ar/^{38}Ar$	±	$^{40}Ar/^{38}Ar$	±	$^{40}Ar/^{38}Ar$	±	$^{40}Ar/^{38}Ar$	±
	1593.77	1.34	1600.24	1.96	1625.76	7.67	1577.95	12.48	1606.37	51.64	1410.08	91.6	1105.81	167.86	1097.03	17
	1614	1.23	1604.26	2.29	1604.56	7.16	1579.56	9.93	1533.66	43.81	1432.79	60.02	1055.65	147.96	1656.38	34
	1608.49	1.33	1610.22	2.43	1618.39	4.32	1604.27	13.97	1592.27	42.28	1581.09	77.27	1982.04	543.76	977.93	11
	1609.75	1.42	1601.48	2.18	1616.19	6.44	1605.08	12.7	1579.97	50.73	1732.52	102.8	2006.36	637.14	1337.71	23
	1606.59	1.49	1599.95	3.34	1613.67	6.25	1599.19	14.71	1591.78	45.32	1897.26	127.61	1243.5	238.71	2084	49
	1615.55	1.67	1601.88	2.42	1598.89	5.47	1584.81	13.06	1552.6	42.78	1610.14	89.48	2035.09	613.68	1435.19	26
	1612.93	1.37	1603.37	2.53	1606.04	7.01	1597.03	12.13	1585.02	39.16	1608.49	86.12	1841.06	439.03	1485.93	29
	1612.13	1.34	1605.97	1.92	1596.85	5.24	1570.72	14.27	1605.16	44.37	1580.82	76.43	1420.77	301.82	1462.66	29
	1614.38	1.33	1607.31	2.79	1620.84	7.21	1616.69	11.86	1597.96	55.59	1442.38	63.65	1236.64	214.53	2123.91	60
	1606.3	1.35	1601.69	2.44	1619.13	6.02	1584.63	11.23	1583.43	42.14	1580.97	91.15	1352.15	232.3	1787.73	35
1-σ	6.4		3.3		9.8		15		23		147		394		378	
1-σ (%)	0.40%		0.21%		0.61%		0.92%		1.5%		9.3%		26%		24%	